Delivery Vehicles for Zerovalent Metal Nanoparticles in Soil and Groundwater

Bettina Schrick, Bianca W. Hydutsky, Jennifer L. Blough, and Thomas E. Mallouk*

Department of Chemistry, The Pennsylvania State University, University Park, Pennsylvania 16802

Received December 19, 2002. Revised Manuscript Received March 11, 2004

Anionic, hydrophilic carbon (Fe/C) and poly(acrylic acid)-supported (Fe/PAA) zerovalent iron nanoparticles were studied as a reactive material for the dehalogenation of chlorinated hydrocarbons in groundwater and soils. The transport of Fe/C nanoparticles was studied by elution through columns packed with model soils from different regions of the USDA soil textural triangle, and was compared to that of unsupported Fe nanoparticles. The Fe/C and Fe/PAA particles form colloidal suspensions that settle very slowly (hours to days) in water. Their anionic surface charge facilitates transport through soil- and sand-packed columns. Elution lengths from column breakthrough studies were compared with calculations based on the Tufenkji−Elimelech model (*Environ Sci. Technol*. **2004**, *38*, 529). It can be concluded from this comparison that nanoparticle diffusion is the dominant filtration mechanism, and that Fe/PAA and Fe/C particles have sticking coefficients on the order of 0.36 and ≤0.07, respectively, in sand and 0.05 and ≤0.01, respectively, in clay-rich Chagrin soil. In contrast, unsupported Fe nanoparticles rapidly agglomerate in water and are efficiently filtered by all of the soils tested, except for the clay-rich soil in which clay platelets may also act as an anionic support material. Trichloroethylene reduction by Pd-catalyzed Fe/C is rapid, and the reaction is unchanged by elution of a suspension of the material through a sand column.

Introduction

Reliable remediation technologies are needed for the decontamination of chlorinated hydrocarbons, which are often introduced into the environment at or below the ground surface. These contaminants migrate through the unsaturated (or vadose) zone, which is the region between the ground surface and the groundwater level, in some cases reaching the underlying saturated zone. As hydrophobic sparingly soluble liquids migrate though the unsaturated zone, they are retained by capillary forces and by adsorption to organic or inorganic colloidal materials in the soil layers.[1] Consequently, sites can have a high concentration of organic contaminants in soil layers in addition to possible groundwater contamination.[2]

It follows that remediation strategies must be tailored for both the unsaturated and groundwater zones. Subsurface remediation methods include soil vapor extraction, pump-and-treat methods, heat treatment, bioremediation, electroosmosis, injection of reactive material (e.g., oxidizers) via hydrofracturing, and the in-situ placement of reactive metal barriers.[1,3,4] All these technologies have their advantages and drawbacks. Their performance depends on several factors, but among the most critical is the ability to access the contaminant in the subsurface.[1]

Newer techniques, such as the injection of reactive slurries or suspended solids, may serve to overcome some of these emplacement limitations so that contaminants at greater depths can be reached and more directly targeted. This can be accomplished by using hydrofracturing,[5] in which pressurized water is injected through wells to develop cracks in impermeable and over-consolidated sediments. The dispersion of microscale iron colloids can also be enhanced, particularly in sandy soils, by using shear-thinning fluids that decrease the local viscosity in soil pores and prevent particle capture by sedimentation.[6] Recently, reactive slurries of nanoscale colloidal Fe−Pd particles have been gravity-fed into an injection well to study the transport and reactivity of the particles in an aquifer.[7]

The dispersion of colloids in soils is affected by particle size, pH, ionic strength, composition of the suspending water, the soil matrix, and flow velocity.[8] Filtration theory, when applied to the problem of colloid transport

* Corresponding author. Phone: 814 863-9637. Fax: 814 863-8403. E-mail: tom@chem.psu.edu.

(1) Buffle, J.; Wilkinson, K. J.; Stoll, S.; Filella, M.; Zhang, J. *Environ. Sci. Technol.* **1998**, *32*, 2887.

(2) Looney, B. B.; Falta, R. W. *Vadose Zone Science and Technology Solutions*, Vol. I & II; Batelle Press: Richland, WA, 2000.

(3) Wong, J. H. C.; Lim, C. H.; Nolen, G. L. *Design of Remediation Systems*; CRC Press/Lewis Publishers: Boca Raton, FL, 1997.

(4) Rumer, R. R.; Ryan, M. E.; *Barrier Containment Technologies for Environmental Remediation Applications*; Wiley & Sons: New York, 1995.

(5) *Hydraulic Fracturing Technology: Applications Analysis and Technology Evaluation Report*; EPA/540/-93/505; U.S. EPA Risk Reduction Engineering Laboratory: Cincinnati, OH; 1993.

(6) Cantrell, K. J.; Kaplan, D. I.; Gilmore, T. J. *J. Environ. Eng.* **1997**, *123*, 786.

(7) Elliott, D. W.; Zhang, W.-X. *Environ. Sci. Technol* **2001**, *35*, 4922.

(8) Nyer, E. K.; Vance, D. B. *Ground Water Monit. Rem.* **2001**, *21* (2), 41−46.

10.1021/cm0218108 CCC: $27.50
Published on Web 04/24/2004

through soils, predicts that particle collisions with the soil matrix are most frequent for very small (<50 nm) and larger (>3 μm) particles, which are prone, respectively, to collection by diffusion and sedimentation mechanisms. Even for particles of optimum size, the collision frequency can be on the order of hundreds per meter.[9] For particles to be effectively transported, almost all of these collisions must be unsuccessful, i.e., the sticking probability must be very low. Controlling the adsorptive properties of particles in soils is thus a key factor in their effective utilization. It is also important to prevent aggregation, which leads to efficient colloid filtration by an interception mechanism.[9] Although it is well-recognized that zerovalent metal nanoparticles are powerful reducing agents for chlorinated hydrocarbons[4,10−16] and reducible metal ions such as Cr(VI)[17−20] and Pb(II),[20] the colloidal chemistry of these particles is such that they tend to aggregate, which prevents their flow through porous media such as soils.

We describe here general-purpose delivery vehicles for soils—anionic hydrophilic carbon and poly(acrylic acid) (PAA)—and demonstrate their effectiveness as carriers for iron nanoparticles. Even though chemical delivery vehicles have become very sophisticated for biomedical applications,[21] they are not often discussed in the context of environmental remediation. A chemical delivery vehicle is a carrier that binds strongly to and transports the reactive reagent, such as a zerovalent metal, to the location where its activity is needed. A chemical delivery vehicle that lowers the aggregation and sticking coefficient of zerovalent metal particles could be particularly useful for contamination sites that cannot be reached easily by hydrofracturing techniques, e.g., under buildings or in urban areas. It could also be helpful for contamination plumes at depths >20 m that cannot be reached by conventional excavation methods.[22] In this paper, we compare the elution of iron nanoparticles on hydrophilic carbon and PAA (hereafter Fe/C and Fe/PAA) to that of unsupported nanoparticles in model soils. We also confirm the reactivity of these supported nanoparticles using trichloroethylene (TCE), a contaminant to which zerovalent metal remediation has been widely applied.

Experimental Section

Synthesis of Hydrophilic Carbon Support and Nanoparticles. The carbon support, Vulcan XC-72 carbon (Cabot Corp.), was made hydrophilic by reaction with the diazonium salt derived from sulfanilic acid. This reaction is thought to decorate the edges and defects of graphitic sheets with covalently linked benzenesulfonic acid groups.[23] An aqueous suspension of 16.8 g of carbon was combined with a solution of 1.2 g of $NaNO_2$ and 2.6 g of sulfanilic acid in water, to which 1.5 mL of concentrated hydrochloric acid was added. The mixture was stirred overnight and the solvent was then evaporated in a crystallizing dish held at 120 °C for 24 h. The resulting black flakes were then Soxhlet-extracted with ethanol for 24 h. The hydrophilic carbon product was analyzed by combustion analysis for C, H, N, and S content, and the surface composition was determined by X-ray photoelectron spectroscopy (XPS).

Supported iron nanoparticles were prepared as described elsewhere for nanoscale zerovalent iron.[24] Briefly, 6.5 g of $FeSO_4 \cdot H_2O$ (Aldrich) and 6.1 g of hydrophilic carbon (Cabot XC-72) or PAA (poly(acrylic acid), Aldrich), average M_w ca. 2000, were combined in 100 mL of deionized water with stirring. In the case of supported Fe−Ni nanoparticles, 1.6 g $NiCl_2 \cdot 6H_2O$ (Aldrich) was also added to the solution. After adjusting the pH to 6.2−7.0 with 3.8 M NaOH, the metal salts were reduced using 4.0 g of solid $NaBH_4$ (Aldrich) which was added in one portion. No precautions were taken to eliminate oxygen from the reaction vessel. Care must be taken when PAA is used as the support, as foaming occurs when the reducing agent is added. A large reaction vessel should be used to avoid foam spillover.

After the $NaBH_4$ was added, the mixture was stirred for 20 min or until visible hydrogen evolution had ceased, and the solid particles were separated from the liquid reaction mixture using a laboratory centrifuge spun at 8000 rpm. The solid product was re-suspended in water, and then in ethanol and acetone to eliminate water. The product was centrifuged each time to separate the solid from the solvent, and finally was dried under vacuum overnight. The same synthetic procedure can be used with other hydrophilic supports, one of which was poly-sodium-4-styrenesulfonate (PSS, 20 wt % in water, Aldrich), average MW 1 000 000. A silica support consisting of 0.60-μm diameter spheres prepared by the Stober method[25] was also used.

The same procedure was used for the synthesis of unsupported iron nanoparticles, except that no support material was added. The unsupported particles were isolated by filtration under Ar using a 0.2-μm-pore-size nylon filter. For the synthesis of supported and unsupported palladium-coated nanoiron (Fe−Pd), a slight modification of the procedure described by Wang and Zhang was used.[26] Nanoiron was prepared using 6.2 g of $FeSO_4 \cdot 7H_2O$ (Aldrich) in 100 mL of deionized water (with pH adjusted to 6.2−7.0 as described above), which was reduced with 3.1 g of solid $NaBH_4$ (Aldrich) in the presence or absence of the appropriate support material. The suspension was then centrifuged, washed with water, and then immediately suspended in a solution of 0.1 g of palladium (II) acetate trimer ($[Pd(C_2H_3O_2)]_3$, 47.5% Pd, Alfa Aesar) in 20 mL of ethanol. This procedure coated the iron surface with Pd via a displacement reaction. The Pd-coated particles were

(9) Logan, B. E. *Environmental Transport Processes*; John Wiley and Sons: New York, 1999; pp 564−613.
(10) Matheson, L. J.; Tratnyek, P. G. *Environ. Sci. Technol.* **1994**, *28*, 2045.
(11) Orth, S. W.; Gillham, R. W. *Environ. Sci. Technol.* **1996**, *30*, 66.
(12) Liang, L.; Korte, N.; Goodlaxson, J. D.; Clausen, J.; Fernando, Q.; Muftikian, R. *Ground Water Monit. Rem.* Winter **1997**, 122−127.
(13) Arnold, W. A.; Roberts, A. L. *Environ. Sci Technol.* **2000**, 34, 1794−1805.
(14) Tratnyek, P. G.; Johnson, T. L.; Scherer, M. M.; Eykholt, G. R. *Ground Water Monit. Rem.* Winter **1997**, 108−114.
(15) Roberts, A. L.; Totten, L. A.; Arnold, W. A.; Burris; D. R., Campbell, T. J. *Environ. Sci. Technol.* **1996**, *30* (8), 2654.
(16) Campbell, T. J.; Burris, D. R.; Roberts, A. L.; Wells, J. R. *Environ. Toxicol. Chem.* **1997**, *16* (4), 625−630.
(17) Boronina, T.; Klabunde, K. J.; Sergeev, G. *Environ. Sci. Technol.* **1995**, *29*, 1511.
(18) Powell, R. M.; Puls, R. W.; Hightower, S. K.; Sabatini, D. A. *Environ. Sci. Technol.* **1995**, *29*, 1913.
(19) Blowes, D. W.; Ptacek, C. J.; Jambor, J. L. *Environ. Sci. Technol.* **1997**, *31*, 3348.
(20) Ponder, S. M.; Darab, J. G.; Mallouk, T. E. *Environ. Sci. Technol.* **2000**, 34, 2564.
(21) Langer, R. *Acc. Chem. Res.* **2000**, *33*, 94.
(22) Powell, R. M., et al. *Permeable Reactive Barrier Technologies for Contaminant Remediation*; USEPA/600/R-98/125; U. S. Environmental Protection Agency, Technical Information Office: Washington, DC, Sept. 1998.
(23) Belmont, J. A.; Amici, R. M.; Galloway, C. P. Reaction of Carbon Black with Diazonium Salts, Resultant Carbon Black Products and Their Uses; U.S. Patent 5,851,280, Dec. 22, 1998.
(24) Schrick, B.; Blough, J. L.; Mallouk, T. E., *Chem. Mater.* **2002**, *14*, 5140.
(25) Stober, W.; Fink, A.; Bohn, E. *J. Colloid Interface Sci.* **1968**, *26*, 62.
(26) Wang, C.-B.; Zhang, W.-X. *Environ. Sci. Technol.* **1997**, *31*, 2154.

Table 1. Textural Composition and Properties of the Model Soil and Sand-Packed Columns

property	Hagerstown (high silt)	Pope (high sand)	Chagrin (high clay)	Ottawa sand
sand %	29.9	55.9	27.7	100
silt %	46.2	25.4	38.0	
clay %	24.0	18.7	34.2	
texture	loam	sandy loam	clay loam	sand
CEC (meq/100 g)	9.2	9.8	17.0	
pH in water	6.2	5.1	7.6	6.9
organic matter %	2.7	3.3	2.8	
dry soil specific gravity (g/mL)	1.12	1.13	0.99	1.52
wet soil specific gravity (g/mL)	1.57	1.53	1.46	1.94
porosity %	45	40	48	42
hydraulic conductivity (m/s)	$(5 \pm 2) \times 10^{-4}$	$(9.0 \pm 0.8) \times 10^{-4}$	$(1.7 \pm 0.2) \times 10^{-3}$	$(2.6 \pm 0.2) \times 10^{-3}$

then centrifuged, washed with ethanol and acetone, and finally dried in a vacuum oven overnight at room temperature.

Physical Characterization. X-ray photoelectron spectroscopy (XPS) was performed on a Kratos XSAM800 pci spectrometer. Nitrogen Brunauer−Emmet−Teller (BET) adsorption isotherms were obtained using a Micromeritics ASAP 2010 surface area analyzer. Iron and boron bulk content were determined using a Leeman Labs PS3000UV inductively coupled plasma spectrophotometer (ICP-AES) at the Penn State Materials Characterization Laboratory. Analysis of samples for C, H, N, and S was carried out by Atlantic Microlabs, Norcross, GA. Transmission electron microscope (TEM) images were obtained at the Electron Microscope Facility for the Life Sciences in the Biotechnology Institute at Pennsylvania State University using a JEOL 1200EXII microscope.

Analytical Measurements. TCE dehalogenation was tested using a purge and trap apparatus (Tekmar LCS-2) coupled to a gas chromatograph (Buck Scientific) equipped with a Restek MXT-502.2 60 m column (0.53 mm i.d., carrier He, 3.0 μm df) and a dry electrolytic conductivity detector (DELCD) sensitive to halogenated compounds. The sample was purged for 6 min in a water bath kept at 35 °C, then desorbed for 5 min at 180 °C. The temperature program for the GC was 40 °C for 5 min, followed by a ramp at 10 °C/min to 200 °C.

Fe−Pd/C suspensions were tested for reactivity before and after elution through sand columns. The stock (5 mg particles/mL) or eluted suspensions, 4 mL, were loaded into 20-mL IChem vials (VWR) with a Teflon mininert valve or a Teflon−silicone septum, which contained 4 mL of 26 ppm TCE in water. The vials were monitored for TCE removal via purge and trap sampling. The reaction vials were rotated on a roller drum about their vertical axis at 11 rpm.

Elution of Supported and Unsupported Nanoparticles through Model Soils. To test the transport of the support materials and particles in model soils, glass buret columns with an inner diameter of 1.2 cm were used. The packing material was either standard Ottawa sand (200−700-mm particle size, E&M Science, CAS 14808-60-7) or one of three soils: Hagerstown, Pope, or Chagrin. These three soils were characterized at the Pennsylvania State University Soil Characterization Laboratory (Table 1). They were stored at 4 °C and passed through a 2-mm-mesh sieve prior to use.

The column ends were equipped with a two-way valve for control of flow rates. A small glass wool plug was pushed to the bottom of each column to prevent drainage of the sand or soil through the column ends. Prior to the addition of nanoparticle suspension, the four columns were slurry-packed to a height of 13 cm. The porosity was measured by comparing the weight of wet and dry soil columns. Porosity and hydraulic conductivity values for these sand and soil columns are given in Table 1. Water used to make the sand or soil slurries and the iron suspensions was first passed through a Nanopure II ion-exchange system, and had a resistivity of 18.3 MΩ−cm and a pH of 6.7.

In the column breakthrough studies, stock solutions of suspended iron nanoparticles (5 mg/mL) were introduced to the top of the column continuously and the eluent was collected in 1.5-mL fractions. For analysis of these fractions in Fe and Fe/PAA experiments, 150-μL aliquots from each fraction were transferred by micropipet into 3.0 mL of an orthophenanthroline (Aldrich, 3 mg/mL) aqueous solution, pH 6.5. Complex formation was quantified by absorbance measured at 508 nm.[27] The dissolution of iron to form the $[Fe(phen)_3]^{2+}$ complex was typically complete within 10 min, as judged from the lack of turbidity of the solution and the constant absorbance reading at 508 nm. Because iron dissolution was rapid, it was not necessary to add HCl. In the case of Fe/C fractions, 2.0 mL of orthophenanthroline solution (3 mg/mL) and 1 mL of 6 M HCl were mixed with each aliquot. The mixture was then centrifuged at 14 000 rpm for 30 min to remove the carbon support. The amount of iron in the supernatant was determined from the absorbance at 508 nm. To ensure that all the iron was removed from the carbon support, fresh orthophenanthroline/HCl solution was added to the carbon pellet. After centrifuging, the supernatant was colorless and no absorbance above background could be detected at 508 nm. The same spectrophotometric methods were used to determine the iron contents of dry Fe/C, Fe/PAA, and Fe−Pd/PAA samples, and of aqueous stock suspensions.

Results and Discussion

Transmission electron micrographs show that the hydrophilic carbon obtained by reaction of Vulcan XC-72 consists primarily of platelets that are 50−200 nm in diameter. These particles are sufficiently large for centrifugal separation, but are much smaller than the average particle sizes of the sand and soils used in our experiments. These carbon particles, either with or without a supported metal, form a persistent suspension in water (settling time > 1 day) because of the negatively charged sulfonate groups that decorate the carbon surface. Elemental analysis and XPS were used to characterize the carbon particles before and after reaction with the diazonium salt derived from sulfanilic acid. The untreated carbon contained 99% C, 0.43% S, and 0% N. After the derivatization, the carbon particles contained 1.61% S and 0.28% N, and the carbon content decreased to 90%. The remaining percentage is most likely oxygen and sodium, which charge balances the sulfonate groups. XPS data confirmed an increase in sulfur on the carbon surface from 0.3 to 1.8%. The surface oxygen content increased by 6%, the sodium content increased by 1.1%, and the carbon content decreased by 9%. The sulfur in the treated samples is oxidized, which is consistent with the presence of sulfonate groups. The sulfonate groups are expected to be located on the edges of the carbon flakes and at defect sites on the basal planes, as has been observed previously for carbon treated with concentrated nitric and

(27) Skoog, D. A.; West, D. M. *Analytical Chemistry*, 4th ed.; Saunders College Publishing: Philadelphia, PA, 1986; pp 612−613.

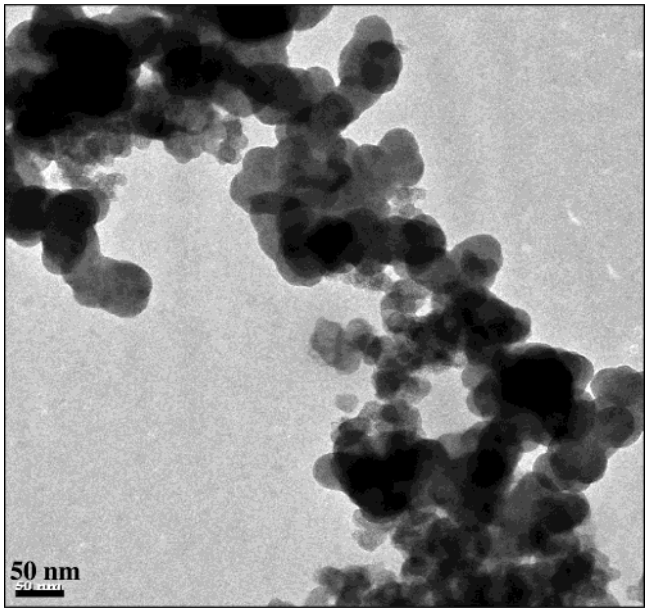

Figure 1. TEM image of carbon made hydrophilic by reaction with the diazonium salt of sulfanilic acid.

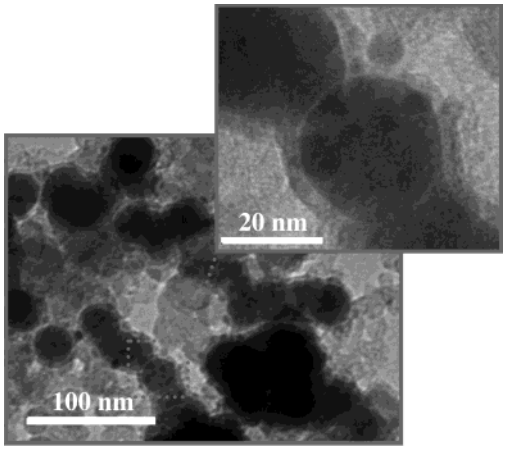

Figure 2. TEM image of hydrophilic carbon-supported iron nanoparticles.

sulfuric acids.[28,29] The strongly acidic sulfonate groups ensure that the carbon particles are negatively charged in the range of pH relevant to soil and groundwater remediation; this high negative surface charge is apparently a key property in preventing the agglomeration of the supported metal particles.

An electron micrograph of hydrophilic carbon particles is shown in Figure 1. A micrograph of Fe/C nanoparticles, Figure 2, shows that the iron exists as 30−100-nm aggregates of smaller primary particles that are enveloped by the sulfonated carbon particles. Because of its lower electron density, carbon appears as a lower contrast material than iron in these images. Lower magnification micrographs showed substantial amounts of free carbon, but little or no iron that was not associated with carbon sheets. From these images it is apparent that there is a strong association between the sheets and the iron particles.

Carbon analysis of the products obtained by borohydride reduction showed that Fe/PAA retained about 2−3% carbon by weight. The surface area of the composite particles, measured by nitrogen adsorption, was typically 20−30 m^2/g. Assuming that most or all of the carbon can be attributed to the strongly adsorbed PAA that remains after washing, the polymer coverage can be calculated. Monolayer coverage of the iron particles by the PAA polymer (about 10^{-5} mol/m^2 on a monomer basis) would correspond to a carbon content of approximately 1 wt %. Therefore, under these conditions, PAA covers the iron particles to the extent of 2−3 monolayers. At a target loading of 21% Fe, a sample of nano-iron supported on sulfanilic acid-treated carbon contained 58% carbon by weight. The support itself contained 90% carbon, so the theoretical carbon content of the Fe/C sample is 71%. The difference can be attributed to small amounts of boron, oxygen, and water that are incorporated into nanoparticles in the borohydride reduction of Fe^{2+}.[24,30]

The dramatic difference in transport of unsupported and carbon-supported metal nanoparticles through sand columns is illustrated qualitatively in Figure 3. Suspensions of hydrophilic-carbon-supported Fe−Ni particles (Fe−Ni/C, 80% carbon) and unsupported particles (Fe−Ni) were made at a 2.5-mg Fe−Ni metal/mL water concentration. A 4-mL portion of each suspension was immediately loaded onto columns packed with Ottawa sand. The unsupported Fe−Ni nanoparticles penetrate less than 1 cm into the column, where they agglomerate and slightly impede the flow of water through the column. The eluent from this column shows no color, indicating that neither iron nor iron oxide penetrates the column. This experiment must be done quickly after making the Fe−Ni suspension, because the nanoparticles tend to agglomerate rapidly when added to water.

In contrast, Fe−Ni supported on hydrophilic carbon passed through the sand almost quantitatively, and had little effect on the gravity flow rate, which in the case of this column was 16 mL/min for the Fe−Ni/C suspension and 19 mL/min for water. The eluent from the Fe−Ni/C suspension is black (Figure 3, right), consistent with elution of most of the particles through the column.

To study the transport of supported nano-iron in more environmentally relevant porous media, soils of diffferent textures were used. These soils were high in either sand, silt, or clay content (Table 1). Hagerstown is rich in silt (size 20−2 μm), whereas Pope soil is rich in sand (size 2−0.2 mm), and both soils have relatively acidic pH. The swelling clay (montmorillonite) fraction of the clay in Hagerstown and Pope soils is only 5%, the balance being primarily kaolinite, illite, and vermiculite. This is consistent with the relatively low pH and low cation exchange capacity of these soils. The Chagrin soil is rich in clay (<2 μm in size) and has a slightly alkaline pH. The order of increasing particle size for the packings based on the percentages of sand, silt, and clay of those samples is therefore: Chagrin < Hagerstown < Pope < Ottawa sand.

The hydraulic conductivities of packed columns of these soils and sand were determined from gravity flow rates (Table 1). In column breakthrough studies with

(28) Hennig, G. R. *Proceedings of the 5th Conference on Carbon*, Vol. I.; Pergamon Press: Oxford, 1962; p 143.

(29) Anderson, J. R. *Structure of Metallic Catalysts*; Academic Press: London, 1975; p 81.

(30) Yiping, L.; Hadjipanayis, G. C.; Sorensen, C. M.; Klabunde, K. J. *J. Appl. Phys.* **1991**, *69*, 5141.

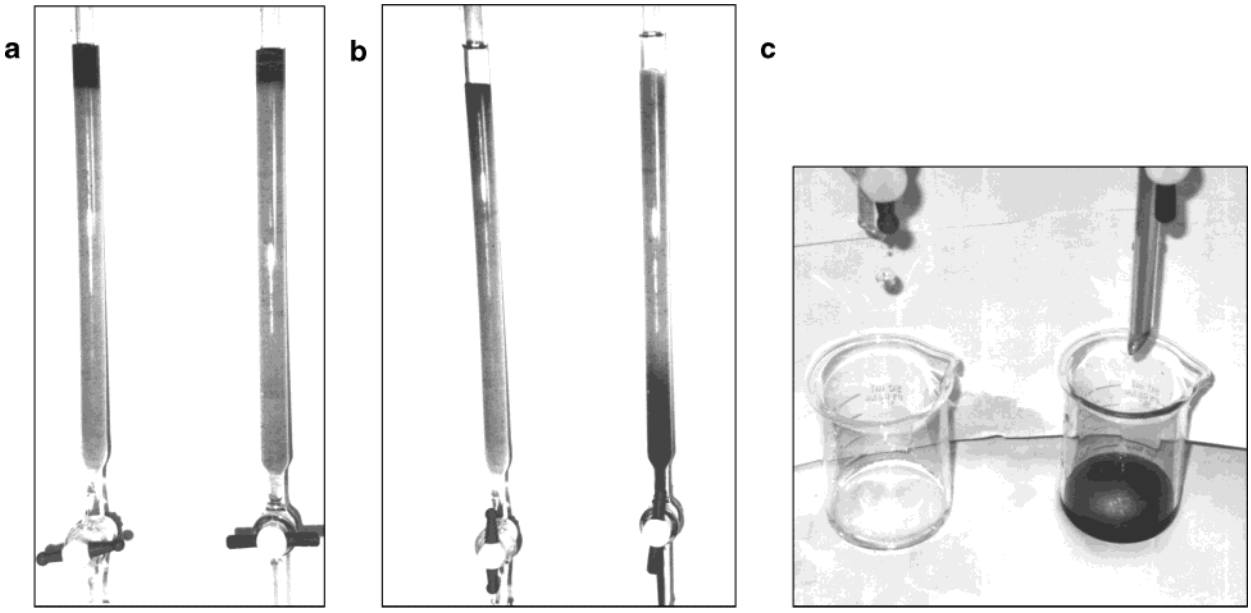

Figure 3. (a) Beginning of nanoparticle elution through Ottawa sand columns: right, Fe−Ni (2.9:1) supported on hydrophilic carbon; left, unsupported Fe−Ni (2.9:1) nanoparticles. (b) Carbon-supported Fe−Ni particles elute with the solvent front (right), whereas unsupported Fe−Ni particles penetrate less than 1 cm into the column (left). (c) Comparison of eluents collected from the two columns. Fe−Ni/C elutes as the original suspension (right), whereas only water passes through the other column (left) because the agglomerated Fe−Ni nanoparticles are strongly retained.

iron nanoparticles, the hydraulic conductivity was dependent on the support material used. The flow rate with Fe/PAA was not significantly different from the water flow rate for any of the soils tested. In sand and Chagrin soil, the flowrate was fast (> 10 mL/min) for water and all of the suspensions. These two packings have very different particle sizes, as the Chagrin soil consists of only 28% sand, the balance being relatively small silt and clay particles. For Pope soil, the flow rate was somewhat slower, but again there was not much difference between the different suspensions. The flow rate of water and of all suspensions was slower (1−5 mL/min, depending on column age and packing conditions) through the silt-rich Hagerstown soil. In this case, the suspended particles impeded the flow of water. This effect was particularly pronounced with the unsupported Fe nanoparticles. For Hagerstown soil, freshly packed columns with relatively fast gravity flow rates (5 mL/min) were used for breakthrough studies.

Breakthrough curves were obtained for 5 mg/mL suspensions of Fe/C, Fe/PAA, and unsupported nanoiron, and the results are shown in Figure 4. In the case of Fe/C, nearly quantitative elution of particles was found for Ottawa sand and Chagrin (high clay) columns, consistent with the results shown in Figure 3. There was minimal elution of Fe/C through Hagerstown and Pope soils. Sand and Chagrin columns retained about 40% of the Fe/PAA injected. In the case of Fe/PAA in Chagrin soil, a downturn of the fraction eluted is observed after several pore volumes (column pore volume = 3−4 mL in each case), suggesting that Fe/PAA particles are retained and ultimately clog the pores in Chagrin soil. Unsupported iron nanoparticles were strongly retained by all the soils tested. Interestingly, unsupported particles eluted most effectively from the Chagrin column, despite the small grain size of the clay-rich soil. This result suggests that some of the anionic clay particles may play a role as supports, much like anionic hydrophilic carbon. It is well-known that clay platelets assist in the transport of cations through soils, particularly at low ionic strength where their electrostatic repulsions are maximized.[31] Clay platelets in water may also increase the effective negative charge on the soil grains through blocking[32] and macromolecular crowding effects.[33]

The reactivity of the Pd−Fe/C particles was unaffected by elution through the sand columns, as shown in Figure 5. The carbon particles by themselves reversibly sorb TCE under these conditions. In groundwater applications involving low concentrations of TCE and other organic contaminants, the carbon support may help to preconcentrate organics for reduction by the supported iron nanoparticles.

The elution of PAA- and carbon-supported iron particles through clay-rich soil and sand is interesting in terms of potential environmental applications. The availability of a soil-permeable support could make the injection and dispersion of colloidal iron and other compounds more efficient, particularly in the remediation of very insoluble and hence immobile contaminants in subsurface deposits that are not easily excavated. However, the relatively poor transport of nano-iron supported on PAA and hydrophilic carbon in low-clay soils (Pope and Hagerstown) presents a potential problem for such applications.

Particle filtration theory can be used to help understand the different transport properties of supported nanoparticles in these soils, and to develop some ideas for improving the particles and supports. There are three basic mechanisms for capture of colloidal particles in porous media: diffusion, which dominates with

(31) Grolimund, D.; Elimelech, M.; Borkovec, M.; Barmettler, K.; Kretzschmar, R.; Sticher, H. *Environ. Sci. Technol.* **1998**, *32*, 3562.
(32) Ryan, J. N.; Elimelech, M. *Colloids Surf., A* **1996**, *107*, 1.
(33) Tohver, V.; Smay, J. E.; Braem, A.; Braun, P.; Lewis, J. *Proc. Natl. Acad. Sci. U.S.A.* **2001**, *98*, 8950.

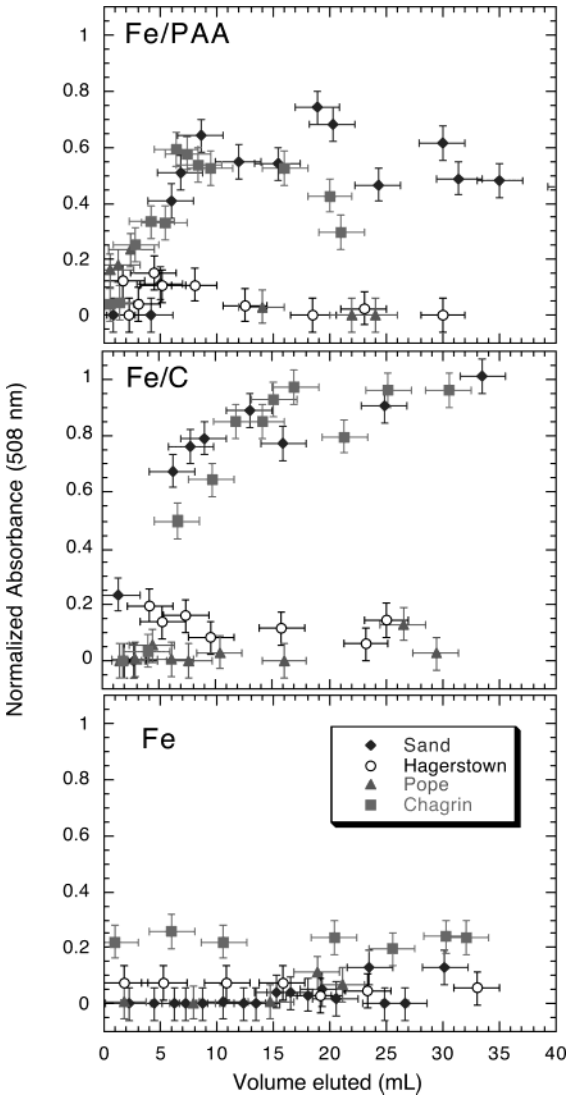

Figure 4. Column breakthrough data for elution of unsupported iron nanoparticles, and nanoparticles supported by PAA and hydrophilic carbon. Each suspension contained 5 g/L solids. Vertical axis shows absorbance at 508 nm of the $[Fe(phen)_3]^{2+}$ complex formed by dissolution and complexation of eluted iron nanoparticle fractions, normalized to the same suspensions before elution.

particles below a few hundred nanometers in diameter, gravitational sedimentation, which dominates with larger particles (particularly those of significantly higher density than water), and interception, which is also important for larger particles and aggregates of primary particles.[9] The additive probability of particle collision by the three mechanisms with the collector grains is the collector efficiency η. The exponential attenuation of particle concentration by filtration is also dependent on the sticking coefficient (α), which represents the fraction of these collisions that are successful in immobilizing a particle.

Early models of particle filtration[34,35] overestimated and underestimated the effects of diffusion and interception, respectively, because they did not accurately consider hydrodynamic and universal van der Waals

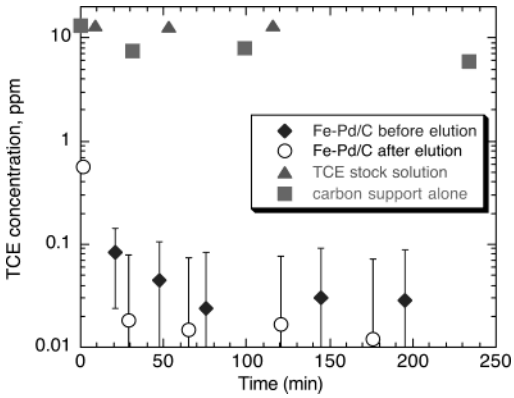

Figure 5. Dehalogenation of 8 mL of 13 ppm TCE using 0.020 g of Fe−Pd/C (20 wt % metal, Fe/Pd atomic ratio 50:1) before and after elution through an Ottawa sand column. TCE is rapidly removed to 20−30 ppb levels. The carbon support itself (0.016 g) adsorbs about 40% of the TCE initially present under the same conditions, but this TCE can be desorbed from the carbon in a second purge-and-trap cycle.

interactions. Recently, Tufenkji and Elimelech (T−E) have re-worked this problem by obtaining an accurate numerical solution to the convection−diffusion equation, which includes these terms.[36] By fitting their results to a power law expression in the same dimensionless parameters used in earlier models, they obtained an accurate expression for collector efficiency:

$$\eta = 2.4A_S^{1/3}N_R^{-0.081}N_{Pe}^{-0.715}N_{vdW}^{0.052} + 0.55A_SN_R^{1.675}N_A^{0.125} + 0.22N_R^{-0.24}N_G^{1.11}N_{vdW}^{0.053} \quad (1)$$

In the T−E equation, the effects of the three filtration mechanisms remain separable: the additive terms represent filtration by particle diffusion, interception, and sedimentation, respectively. The dimensionless parameters A_S, N_R, N_{Pe}, N_{vdW}, N_A, and N_G can be calculated from the soil porosity, particle size, soil grain size, Darcy (or superficial) fluid velocity, particle density, fluid temperature and viscosity, and particle Hamaker constant.[37] This equation has been successfully used to fit a large body of literature data on particle transport through porous media. Although the model should be applied cautiously to real soils (which contain a range of grain sizes), it can nevertheless be used to obtain an estimate of filtration lengths and to understand the effects of particle size and flow rate on transport.

In the "clean bed" limit, in which adsorbed particles do not cover an appreciable fraction of the surface of the porous medium, the particle concentration N decays

(34) Yao, K.-M.; Habibian, M. T.; O'Melia, C. R. *Environ. Sci. Technol.* **1971**, *5*, 1105.
(35) Rajagopalan, R.; Tien, C. *AIChE J.* **1976**, *22*, 523−33.

(36) Tufenkji, N.; Elimelech, M. *Environ. Sci. Technol.* **2004**, *38*, 529.
(37) The porosity function A_S is defined as $A_S = (2(1 - \gamma^5))/(2 - 3\gamma + 3\gamma^5 - 2\gamma^6)$, where $\gamma = (1 - \theta)^{1/3}$. The Peclet number $N_{Pe} = Ud_c/D_p$, where $D_p = k_BT/(3\pi\mu d_p)$. U is the superficial (or Darcy) flow rate, k_B is Boltzmann's constant, T is the absolute temperature, and μ is the fluid viscosity. The other parameters are given by $N_{vdW} = A/k_BT$, $N_A = A/2\pi d_p^2\mu U$, $N_R = d_p/d_c$, and $N_G = d_p^2g\Delta\rho/18\mu U$, where A is the particle Hamaker constant, g is the gravitational constant, $\Delta\rho$ the difference in specific gravity between the particle and the fluid, and d_p and d_c are the particle and soil grain diameters, respectively. See ref 36 for complete details. For iron nanoparticles, we used $\Delta\rho = 6$ g/cm^3, $A = 1 \times 10^{-20}$ J, and $T = 288$ K. Variation of these parameters within reasonable limits did not significantly affect the results shown in Figure 6.

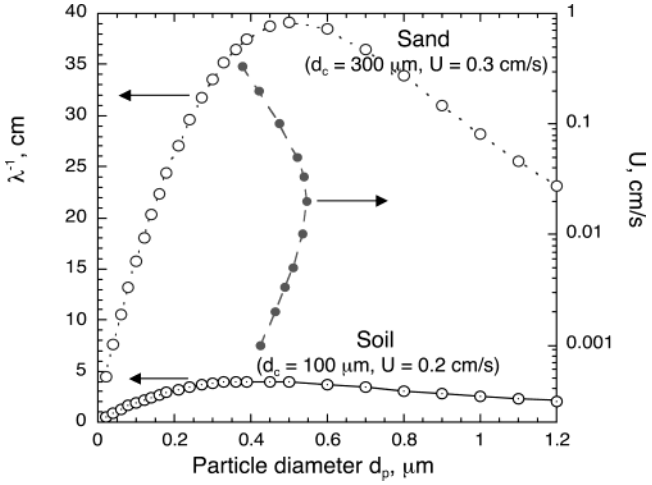

Figure 6. Open circles: Calculated filtration length (λ^{-1}) as a function of iron particle diameter, d_p, from eqs 1−3. Upper curve shows a calculation for Ottawa sand (porosity $\theta = 0.42$, $d_c = 300$ μm, Darcy flow velocity $U = 0.3$ cm/s). Lower curve shows a calculation for an average soil ($\theta = 0.42$, $d_c = 100$ μm, $U = 0.2$ cm/s). Filled circles: Particle diameter with maximum calculated value of λ^{-1} as a function of Darcy flow velocity for soil ($\theta = 0.42$, $d_c = 100$ μm).

exponentially according to eq 2

$$\ln\left(\frac{N}{N_0}\right) = -\alpha\lambda L \tag{2}$$

where N_0 is the concentration at the inlet and L is the distance traveled through the column.[9] The filtration constant, λ, may be calculated from η by using eq 3, in which θ is the column porosity and d_c is the collector (or grain) size of the soil.

$$\lambda = \frac{3}{2d_c}(1-\theta)\eta \tag{3}$$

Figure 6 shows a calculation of the filtration length $(\lambda)^{-1}$ vs particle size from eqs 1−3 under the conditions of our experiments for sand ($d_c = 300$ μm) and soil ($d_c = 100$ μm) columns. The filtration length corresponds to the column length at which the particle concentration falls to $1/e$ of its initial value if the sticking coefficient $\alpha = 1$. Experimentally, α may be obtained by comparing experimental filtration lengths $(\alpha\lambda)^{-1}$ with calculated λ^{-1} values.

By comparing the results shown in Figures 3, 4, and 6, one may draw two important conclusions. First, sticking coefficients are lower than unity for Fe/PAA and Fe/C in Ottawa sand and Chagrin soils. We can estimate α for Fe/PAA in Ottawa sand from the observation that about 60% elutes from a 13- cm column. Using eq 2, we obtain $(\alpha\lambda)^{-1} \approx 25$ Å. From Figure 6, using $d_p \approx 50$ nm, the calculated λ^{-1} value is 9.1 cm, and therefore $\alpha \approx 0.36$. Similarly, for Fe/PAA in Chagrin soil ($\lambda^{-1} \approx 1.1$ cm), we can estimate $\alpha \approx 0.05$. For unsupported iron nanoparticles in Chagrin soil, $\alpha \approx 0.14$, because the observed elution of 20% implies $(\alpha\lambda)^{-1} \approx 8$ Å. For Fe/C in sand and Chagrin soil, the nearly quantitative elution from 13-cm columns implies α values ≤ 0.07 and ≤ 0.01, respectively. In general, α values are lowest for Chagrin soil, which has the highest cation exchange capacity and therefore the highest negative surface charge density. This is consistent with the idea of repulsive interactions between the negatively charged support materials and negatively charged soil grains.

The second important conclusion one can draw, particularly from Figure 6, is that the filtration of nanoparticles is dominated by diffusion, and better transport can be anticipated for larger particles. The particles studied in our experiments (30−100 nm diameter) appear at the extreme low end of the plots in Figure 6. For 50-nm iron nanoparticles in sand, for example, we calculate a filtration length of 9 cm, whereas for 0.5-μm particles, the filtration length is 39 cm. Under the conditions shown in Figure 6, the optimum particle size is 0.40−0.50 μm for both sand and soil columns. The fact that the maximum in calculated elution length is roughly independent of grain size and flow rate seems counterintuitive; it can be explained by the fact that the probability of particle filtration by both the diffusion and interception mechanisms increases as the grain size decreases. Although particle collection by the diffusion mechanism is more sensitive to flow rate than is collection by interception, the optimum particle diameter varies between narrow limits of 0.38 and 0.55 μm for all reasonable values of Darcy flow velocity ($U \geq 0.003$ cm/s).

Conclusions

Anionic support materials such as hydrophilic carbon and PAA inhibit aggregation and significantly reduce the sticking coefficient of iron nanoparticles in Ottawa sand and in a high-clay soil. The relatively poor transport of these particles in the other soils tested implies a higher sticking coefficient with lower soil charge density. The calculation of filtration lengths using the T−E model shows that 30−100 nm diameter particles will have poor transport properties compared to particles that are 400−500 nm in diameter. Unfortunately, larger particles tend to have lower reactivity because their surface area per unit mass scales inversely with particle diameter. This suggests that the immobilization of nanoparticles on submicron support media should give optimum transport and reactivity. Experiments that explore this idea are currently in progress.

Acknowledgment. This work was supported by National Science Foundation grant CHE-0095394. We thank Dr. Rosemary Walsh and the Electron Microscope Facility for the Life Sciences in the Biotechnology Institute at Pennsylvania State University for the use of the transmission electron microscope. We thank Brian Kelley for help with obtaining TEM images. We thank Dr. Mark Strynar and Prof. Jean-Marc Bollag for providing the three model soils that were used for the elution experiments. We also thank Prof. Bruce Logan for very helpful discussions of particle filtration theory.

Note Added after ASAP Posting

This article was released ASAP on 4/24/2004. Subsequently, a sentence in the Conclusion was modified, and the revised version was posted on 4/30/2004.

CM0218108